

*Library L. M. G. L.*

TECHNICAL MEMORANDUMS

NATIONAL ADVISORY COMMITTEE FOR AERONAUTICS

---

No. 689

---

THE PROBLEM OF TIRE SIZES FOR AIRPLANE WHEELS

By Franz Michael

Zeitschrift für Flugtechnik und Motorluftschiffahrt  
Vol. 23, No. 13, July 14, 1932  
Verlag von R. Oldenbourg, München und Berlin

---

Washington  
October, 1932

NATIONAL ADVISORY COMMITTEE FOR AERONAUTICS

TECHNICAL MEMORANDUM NO. 689

THE PROBLEM OF TIRE SIZES FOR AIRPLANE WHEELS\*

By Franz Michael

INTRODUCTION

Several years ago the development of high-pressure tires seemed to have reached the stage where international standardization of airplane tires and wheels was about to be achieved. Now the sudden change to balloon or low-pressure tires, brought about by the American experiments with low-pressure tires, has brought this development to a full stop. Efforts at a tentative international standard for wheel hubs are under way, to facilitate an exchange of wheels. But any attempt at standardization of wheels should begin with the tires, because, after all, the shape of the tire is of decisive importance for the design of wheels, brakes and wheel hubs.

For that reason it seems extremely timely to raise the question of best tire sizes for airplane wheels. Specifically, it is appropriate to obtain to a comprehensive survey of the influence of different size tires on its qualities in order to be better able to pass upon any proposed new designs.

At the present time every country is engaged in designing new tire series which, after all differ but little from each other in many respects.

On the basis of experiments and theoretical considerations a proposal is made for a standard tire series for airplane wheels, without regard to existing standards. It is only with an ideal classification, as it were, that a comparison with the already existing standard proposals has any proper meaning.

---

\* "Zur Frage der Abmessungen von Luftreifen für Flugzeuglaufräder." Z. F. M., July 14, 1932, pp. 377-390.

## NOTATION

- A, (mkg) energy absorption of tire loaded to arbitrary deflection  $\lambda$ .
- $A_g$ , (mkg) energy absorption of tire loaded to deflection  $\lambda_g$ .
- $A_{g_1}$ , (mkg) energy absorption of a shock absorption system loaded to maximum elastic travel  $f_{g_1}$ .
- b, (cm) width of tire, i.e. diameter of tire cross section.
- $b_T$ , (cm) width of brake drum.
- D, (cm) outside diameter of tire.
- $D_T$ , (cm) diameter of brake drum.
- F, (cm<sup>2</sup>) ground pressure area of tire under arbitrarily assumed wheel load; i.e. area of contact of tire by which the bearing pressure is transmitted to a level supporting surface.
- $F_e$ , (cm<sup>2</sup>) area of contact of tire approximated as ellipse.
- $F_e^1$ , (cm<sup>2</sup>) area of contact of tire when tire deflection  $\lambda = \lambda_e$ .
- $F_b$ , (cm<sup>2</sup>) braking surface of wheel brake, i.e. total area of brake bands.
- f, (cm) elastic travel of tire under arbitrary perpendicular loading of wheel axis.
- $f_g$ , (cm) maximum travel possible by air shock absorption, i.e. deflection of tire to the rim.
- $f_r$ , (cm) elastic travel under load, i.e. travel under static tire load as result of airplane weight.

- $f_1, f_r, f_{g_1}$ , (cm) corresponding travel of shock absorber, i.e. landing gear shock absorption additive to that of tire.
- $h$ , (cm) height of obstacle.
- $N$ , ( $\frac{\text{mkg}}{\text{s cm}^2}$ ) specific braking power of brake bands of wheel brake.
- $n = \frac{P_g}{P_r}$ , safe impact factor of tire, i.e. quotient of tire loading when  $\lambda = \lambda_g$  and wheel load ( $\lambda = \lambda_r$ ).
- $P$ , (kg) tire loading.
- $P_r$ , (kg) maximum permissible static load on tire due to gross weight of airplane.
- $P_g$ , (kg) maximum loading of tire, i.e. when  $\lambda = \lambda_g$ .
- $P_1, P_r, P_{g_1}$ , (kg) corresponding forces of the shock absorber.
- $P_b$ , (kg) braking action, i.e. force of deceleration transmitted to airplane with complete braking of wheel.
- $p$ , (atm.) air pressure of air-inflated tire under arbitrary deflection  $\lambda$ .
- $p_0$ , (atm.) inflation pressure, also air pressure by  $\lambda = 0$ .
- $\bar{p}, \bar{p}_0$ , (atm.) absolute pressures ( $\bar{p} = p + 1$ ).
- $\Delta p = p - p_0$ , (atm.) rise of air pressure under loading of tire with arbitrary wheel loads.
- $u = \frac{F_e}{b^2}$ , coefficient for defining area of contact approximated as ellipse.
- $V = \frac{u}{\lambda_e - 0.03}$ , form coefficient defining the load absorption.
- $v$ , (m/s) rate of rolling of airplane at start of first full brake action of a braked landing.

- $\delta$ , degree of utilization of brake drum area with given brake band arrangement.
- $\epsilon = \frac{b_T}{D_T}$ , relative width of brake drum.
- $\zeta$ , correction factor for sidewall stiffness of tire to define the load absorption from area of contact and air pressure in tire.
- $\eta$ , ratio of available to maximum energy of shock absorption diagram.
- $\kappa$ , coefficient for defining rise of air pressure in tire.
- $\lambda = \frac{f}{b}$ , tire deflection due to arbitrary tire loading  $P$ .
- $\lambda_r = \frac{f_r}{b}$ , tire deflection due to static loading  $P_r$ .
- $\lambda_g = \frac{f_g}{b}$ , maximum possible tire deflection.
- $\lambda_e$ , tire deflection, at which the actual area of contact equals the contact area approximated as ellipse.
- $\phi = \frac{D}{b}$ , form ratio of a tire.

#### ELASTIC QUALITIES OF TIRES FOR AIRPLANE WHEELS

The tire of an airplane wheel represents an air cushion within a rubberized fabric casing. The inherent stiffness of the rubber casing, compared with that of the customary automobile tire of similar size, is very low. Consequently it should be possible in simple fashion to determine the load absorption of an airplane tire of any size with sufficient accuracy by calculation from the given data on air volume and inflation pressure (initial air pressure in inner tube).

As basis hereto, various load test series were to be used. Proceeding from earlier experimental results we introduce the following quantities as typical values of an airplane tire, that is, as independent variables:

Tire width  $b$ , as criterion of tire size and of elastic travel of tire.

Form ratio  $\phi = \frac{D}{b}$ , as criterion of the type of design.

Inflation pressure  $p_0$ , as criterion of the change in elastic properties (load absorption for given tire size)

At the same time we express the elastic travel of the wheel axis relative to a load as the ratio  $\lambda = \frac{f}{b} = \frac{\text{elastic travel}}{\text{tire width}}$ , and call it "tire deflection."

We began with loading experiments on a level supporting surface, static in the compression press and dynamic in the drop hammer.

# 1. LOADING TESTS TO DETERMINE THE LOAD ABSORPTION ON A LEVEL SUPPORTING SURFACE

## Test Procedure

In order to gain an insight into the behavior of different tires it was necessary to make these tests with special tires of widely varying form ratio. We had at our disposal several tires with flat base rim of a German standard series and two American low-pressure tires of the Goodyear Tire and Rubber Company, whose hubs also conformed in design to the flat base rims of the high-pressure wheels.

TABLE I. EXAMINED AIRPLANE TIRES

Tire sizes mm	$\phi$ For nominal sizes	Dimensions		Applied inflation pressure $p_0$ in atm.
		D x b mm	$\phi$	
22 x 10 - 4	2.2	565 x 250	2.26	0.5; 1; 1.5; 2
30 x 13 - 6	2.31	755 x 328	2.3	0.5; 0.75; 1; 1.5; 2; 3
1,300 x 300	4.33	1,270 x 318	4.0	1; 3; 4; 5
1,100 x 220	5.0	1,115 x 225	4.95	1; 3; 4; 5
810 x 125	6.48	800 x 126	6.35	1; 2; 3; 4; 5
760 x 100	7.6	749 x 99	7.57	2; 3; 4

mm x .03937 = inches

5.0 ✓  
4.5 ✓  
4.5 ✓  
4.0 ✓

The table contains the nominal as well as the actual sizes defined by applying the usual inflation pressures, and the inflation pressures themselves. Accordingly the form ratio is given with respect to the nominal and to the actual sizes. For all subsequent purposes only the actual tire sizes are used as basis. Conformably to the appended inflation pressures the experiments were extended to unusually high pressures on the low-pressure tire and to low pressures on the high-pressure tire.

The loadings were applied as static loads with different inflation pressures up to touching of the rim, in addition to drop tests in the DVL 3-ton drop hammer, from different heights and with a given inflation pressure. The drop weights were so chosen that, on impact, the tire practically deflected to the rim.

Area of contact with the supporting surface, air pressure in tire, load on wheel and elastic travel were defined in the static tests. Owing to the subordinate role of the stiffness of the thin protector of the airplane tires, the data on the area of contact, obtained by imprint of the blackened tire on chalk-covered paper, were of great importance. In the strict sense of the word these contact areas are valid only for loading on a level, hard, and comparatively smooth surface. The rate of loading was approximately one minute per stage. From the measured elastic travel the tire deflection  $\lambda$  relative to the actual tire width was then determined. The dynamic tests were intended to supply a dynamic diagram comparable to the static shock absorption diagram, so as to afford the percentage deviations between both types of loading. In this manner the dynamic qualities of the tire are readily estimated from a very easily determinable static diagram by corresponding percentaged additions.

The drop-hammer test yielded shock force and elastic travel with respect to time, height of drop and rebound, and, in several cases, the number of bounces up to complete rest position of hammer.

#### Results of Tests

In Figure 1 the area of contact has been plotted against tire deflection  $\lambda$  for all tires. It rises linearly for all tires up to about  $\lambda = 0.5$ , above it, the tires with small form ratio  $\phi$  lag behind relative to the

7

straight rise, whereas the tire with large form ratio, as the 760 x 100 size for example, maintains this straight rise until it almost rides on the rim.

The rise of the air pressure in the tire is most readily portrayed by plotting the ratio of pressure rise  $\Delta p$  to absolute inflation pressure  $\bar{p}_0$  in logarithmic scale against deflection  $\lambda$ . (Figs. 2, 3, and 4.) It is seen that the curves (aside from a few values, especially by small deflection) are fairly straight, so that representation by simple exponential function is admissible. As concerns the dependence on the chosen inflation pressure itself, it was found that the ratio  $\frac{\Delta p}{\bar{p}_0}$  deviates somewhat stronger at very low air pressure, whereas the test points, at higher air pressure in the tire, are practically coincident in one single curve. It is noteworthy that here also the balloon tire fits perfectly among the other tires.

Some of the load absorption curves of the static tests are reproduced in Figures 5, and 6. They manifest the well-known slightly curved aspect. Below these curves is the corresponding air pressure in the tires. The damping obtained under static load, defined as the ratio of  $\frac{\text{lost energy}}{\text{absorbed energy}}$  during one load cycle averaged

9 per cent for the high-pressure tires, and  
12 " " " " low-pressure tires.

The curves for the other tires, being similar, were omitted.

The dynamic tests yielded the following. Even a drop test from very low height already reveals a greater (although not appreciable) energy absorption than in the static test. Increasing the height of drop and choosing the weight such as to approximately use up (to about  $\lambda = 0.7$ ) the maximum elastic travel of the tire available during the test results in a very unessential change in the load-travel curve previously recorded for low height of drop, so long as the particular height up to 1 m, or 4.5 m/s shock rate, is not exceeded. Figure 7 shows the load absorption of the 30" x 13" (762 x 330) American tire in drop hammer test at different shock rates plotted against the elastic travel.



## DATA OF DROP TEST

Figure 7	Height of drop	Inflation Pressure $P_0 = 1.25$ atm.	
		Weight of hammer	Rate of drop when hitting
$\Delta$	0 cm	2,217 kg	0 m/s
$\times$	16.3 "	1,343 "	$\sim 1.8$ "
+	49.7 "	734 "	$\sim 3.1$ "
$\square$	68.2 "	565 "	$\sim 3.7$ "
$\circ$	88.4 "	480 "	$\sim 4.2$ "
	Height of drop	Inflation Pressure $P_0 = 0.5$ atm.	
		Weight of hammer	Rate of drop when hitting
$\Delta$	0 cm	1,308 kg	0 m/s
$\times$	15.4 "	710 "	1.7 "
$\circ$	44.3 "	480 "	3.0 "

cm  $\times .3937 =$  in.    kg  $\times 2.20462 =$  lb.    m/s  $\times 3.28083 =$  ft./sec.

We only show the curves of the static loading and those of the drop test from maximum height, and a few selected data from the intermediate tests. It is seen that within range of the employed shock rates, the load-travel curves show a discrepancy only under small deflections, that is, they approach in this range at small shock rates, the load-travel curve of the static test. The other tires showed the same behavior, hence reproduction of the curves is superfluous. The absorption of force under dynamic loading at shock rates up to 4.5 m/s was from 6 to 15 per cent higher than under static loading, wherein the low figures are for the high-pressure tire and the high figures for the low-pressure tire with very low inflation pressure. The discrepancy between the dynamic and the static damping is minor, although it is ordinarily a little higher in the dynamic test. As concerns the shock figures, the 810  $\times$  125 and the 30"  $\times$  13" (762  $\times$  330) tire for example yielded the figures appended in Table II.

TABLE II. NUMBER OF DROPS

Tire	Height of drop cm	Falling weight kg	Inflation pressure atm.	Number of drops
810 x 125	10.1	660	3.0	16
	14.7	565	4.0	20
	15.6	710	0.5	14
30" x 13"	14.0	928	0.75	17
(762x330)	15.7	1,503	1.5	23

The quoted figures are merely intended as an approximate picture for the two tires under approximately identical test conditions. A more searching investigation within the scope of this report is superfluous because the influence of the principal dimensions of the tire on the damping was found to be inferior. Another fact to be remembered is that the dynamic tests had to be limited to the nonrolling wheel, so that the plotted curves of the dynamic tests have a more theoretical aspect. At the same time, no conclusions should be drawn from the damping obtained by the static test about the damping by rolling wheel.

## 2. DEFINITION OF POWER ABSORBED

The loading experiments revealed, as anticipated, that by selection of correct reference quantities, even the low-pressure tires that differ so much in shape and inflation pressure, align themselves consistently in their behavior into the series of the other tires. Consequently it is justified to deduce an approximation formula for computing the load absorption of any tire based upon the experimental results of the preceding chapter. To define the elastic properties of any tire the data for the static load absorption suffice for practical cases. With this information the other values are readily estimated on the basis of the test data for ordinary airplane tires.

a) Development of Approximation  
Formula for Load Absorption

The pertinent test data necessary hereto are:

1. The increase in contact area must be sufficiently proportionate to the tire deflection.
2. The rise of air pressure in the tire must be sufficiently proportionate to the product of absolute inflation pressure and square of tire deflection.
3. The product of contact area and air pressure by given deflection must obtain to a sufficiently accurate conclusion of the static vertical loading on the tire.

We begin with the contact area dependent on the tire deflection. Instead of the actual contact area, we determine the area of the approximated ellipse as shown in Figure 8.

Assuming a certain deflection  $\lambda < 0.5$ , and with the fact in mind that

$$\frac{D}{b} = \varphi \text{ and } \frac{f}{b} = \lambda$$

we obtain

$$F_e = \pi \lambda b^2 \sqrt{(\varphi - \lambda)(1 - \lambda)}$$

This approximation of area of contact by an ellipse is very crude for a large range of the deflection. In fact, it loses all practical significance as approximation when  $\lambda > 0.6$ . But there is one deflection  $\lambda_e$  for each tire size, at which the area of ellipse  $F_e$  equals the actual contact area  $F$ , and to define it we determine the area of ellipse  $F_e$  for deflection  $\lambda = 0.4$  to  $\lambda = 0.65$ .

To facilitate the calculation of the ellipse we put

$$F_e = u b^2$$

and plotted the value

$$u = \pi \lambda \sqrt{(\varphi - \lambda)(1 - \lambda)}$$

in Figure 9 against the form ratio  $\phi$  for different values of tire deflection  $\lambda$ .

The curves for  $F_e$  obtained on the basis of Figure 9 are shown in Figure 1. Then the actual contact areas were approximated by straight lines and it was found that these lines could be satisfactorily combined into one group by a slight zero point displacement for  $\lambda = 0.03$ .

The intersection of the  $F_e$  with the  $F$  curve reveals deflection  $\lambda_e$ , i.e., that at which  $F$  equals  $F_e'$ , the contact area of the ellipse. Thus Figure 1 yields for the actual area of contact the following equation:

$$F = F_e' \frac{\lambda - 0.03}{\lambda_e - 0.03},$$

with  $F_e' = u b^2$  substituted for  $\lambda = \lambda_e$  and  $F = 0$  for  $0 < \lambda < 0.03$ .

And together with the terms that depend only on  $\lambda_e$  and thus on  $\phi$ , the contact area finally becomes

$$F = V (\lambda - 0.03) b^2$$

wherein the form coefficient

$$V = \frac{u}{\lambda_e - 0.03}$$

was defined by experiment and plotted in Figure 10 against form ratio  $\phi$ .

Now we examine the rise in air pressure. In Figures 2 to 4 the curves for the pressure rise, that is, the ratio

$\frac{\Delta p}{p_0}$ , have been replaced by straight lines, the straight lines of the approximation fairly representing the usual pressures for the respective tire. This yields as approximation for the pressure rise the equation

$$\frac{\Delta p}{p_0} = k \lambda^2$$

The factor  $k$  denotes the pressure ratio  $\frac{\Delta p}{p_0}$  for ideal deflection  $\lambda = 1$ . Figure 11 shows these  $k$  values

plotted against form ratio  $\phi$ . It results in a curve with pronounced rise as  $\phi$  diminishes. One feature of the diagram is the marked rise of the air pressure in the low-pressure tires, one of the chief arguments advanced in their favor.

The air pressure at any deflection is:

$$p = p_0 + \bar{p}_0 \kappa \lambda^2$$

and the load absorption is approximately correct at

$$P = \zeta p F$$

with  $\zeta$  = correction factor for the influence of stiffness of the tire walls. With zero stiffness,  $\zeta = 1$ , i.e., the contact pressure would be evenly distributed across the whole contact area and would exactly correspond to the air pressure at every point.

But in reality, there is a certain stiffness, which by low air pressure especially is anticipative of greater load absorption than corresponds to the product air pressure  $\times$  area of contact. It is seen that within ambit of the present approximation it suffices to show the correction factor  $\zeta$  solely as function of the air pressure in the tire. For the discrepancies in stiffness from the point of view of chosen tire wall thicknesses are, after all, not very essential in a change from high to low pressure type. Several experimentally defined  $\zeta$  are shown in Figure 12, plotted against the inflation pressure. To define these values we substituted the measured values for different deflections in place of load absorption, contact area and air pressure, and formed an average value of  $\zeta$  for each loading experiment. The thus obtained  $\zeta$  values were traced in Figure 12 and approximated by a curve. It is seen that for pressures above 3 atm. the discrepancy of the load assumption from the product  $p F$  is only a few per cent and wholly within the order of magnitude of measuring accuracy. At pressures between 0.5 and 1 atm. on the other hand, the discrepancy already ranges between 10 to 20 per cent. For  $p_0 = 0$ ,  $\zeta$  must  $= \infty$ , because of the existence of load absorption due to tire stiffness, despite the absence of inner negative pressure.

At last the final approximation formula for load absorption reads

$$P = \zeta v b^2 (p_0 + \bar{p}_0 \kappa \lambda^2) (\lambda - 0.03)$$

wherein

$\zeta = f(p_0)$  to be taken from Figure 12

$V = f(\varphi)$  " " " " " 10

$\kappa = f(\varphi)$  " " " " " 11

An illustrative example of load absorption computed according to this formula is afforded in Figure 13, which was carried out on a 1,100 X 220 tire, on the basis of the nominal sizes and of the permissible maximum deviations for diameter and tire width conformably to the German tentative standard DIN L19. We included two other curves from two different 1,100 X 220 tires for comparison. The hatched zone corresponds to the change in load absorption already possible by admissible dimensional deviations. Of course, this zone becomes smaller if the absolute elastic travel is chosen as abscissa instead of the deflection.

In order to facilitate the determination of the energy absorption of any given tire the approximation formula is graphically shown in Figure 14. It yields the static tire loading for any deflection  $\lambda$  by given form ratio  $\varphi$ , inflation pressure  $p_0$  and tire width  $b$ , so that the desired load absorption curve by eventual interpolation for intermediate inflation pressure can be forthwith plotted.

#### b) Limits of Approximation Formula for Absorption of Energy

Because of the proportionality between area of contact and deflection throughout the entire range up to maximum deflection  $\lambda_g$  stipulated in the development of the approximation formula, the latter indicates unduly high values for the tire load in vicinity of  $\lambda = \lambda_g$ , especially for tires with small form ratio  $\varphi$ , a fact which must be kept in mind when determining the possible total energy absorption of the tires.

The extent of the influence of the admissible deviations of tires from the nominal sizes on the amount of load absorption is readily manifested by the calculated curves of Figure 13. Besides these deviations in size there is the influence of the tire form itself, as, for example, the

amount of rim diameter with given tire diameter. The direct influence of a larger rim diameter on the load absorption should not be very great. The absorption curve would simply be bounded by a lower maximum deflection  $\lambda_g$ . On the other hand, it should be remembered that a change in rim diameter is now and then bound up with a material change in available total air volume. To be sure, one will strive to maintain a sufficient air volume by appropriate design of rim base, as in the case of "streamline tires." In any case, the application of the approximation formula to tires with markedly deviating rim shape should be accompanied by a check on whether the area of the tire inner cross section (section of cylindrical air volume) referred to tire width  $l$  is in approximate agreement with the cross-sectional area of the examined conventional tires with flat-base rim. Since the amount of air volume is decisive for the rise in air pressure, marked deviations by moderate changes in rim shape are not anticipated except with tires of very low inflation pressure, where the rise in air pressure exerts a marked effect on the absorption of energy. As to the stiffness, no serious divergence from the computed energy absorption curve is expected, unless the tire has essentially stiffer walls, such as an especially heavy protective casing, for instance.

### 3. RISE IN WHEEL FORCE WHEN ROLLING OVER AN OBSTACLE

One decisive advantage of the low-pressure tire is its excellent rolling qualities on uneven ground. Now it becomes especially important to determine what definite quantities of the airplane tires primarily influence these rolling characteristics. Such an investigation really should be made on predicated assumptions of landing gear arrangement, mass distribution etc., although a few elementary experiments suffice to give a qualitative picture of the conditions. Assume the airplane, fully loaded, rolls over perfectly level ground. Then the wheel center moves at constant distance from the ground, corresponding to tire deflection  $\lambda_r$ ; force of tire and load on wheel are in equilibrium. Now a roll over a small obstacle upsets this equilibrium, insofar as the wheel force, due to the changed contact area and tire deformation increases because of the obstacle. The result of this increase is a fluctuation of the airplane mass depending on the softness of the tire and on the shock absorber. Next assume that the airplane does

•

not diverge when passing over the obstacle. Then the force of the wheel increases, but only as affected by the tire size, which is a specific property of the tire. There is no doubt but that that tire is the best which shows the smallest increase in force in such a test, because then no marked disturbance in rolling equilibrium of the free rolling airplane is to be expected.

In order to simplify the experiment we statically tested the airplane wheel with different obstacle settings up to  $\lambda_r = 0.3$  relative to level supporting surface, instead of measuring the force with rolling wheel. (Loading period about 2 minutes.) As obstacle we used two round pieces of timber 20 and 40 mm high. Figure 15 shows the two tires, 810 X 125 and 30" X 13" (762 X 330) in the large obstacle test; Figure 16, divers areas of contact of the same tires at different settings of the large obstacle.

In this obstacle test we defined the ratio of the wheel force with obstacle ( $P$ ) and without obstacle ( $P_0$ ) for the same load deflection  $\lambda_r$ , as illustrated in Figures 17 and 18. The experiments revealed that the maximum increase does not lie in the center. In these static tests the wheel force increment is symmetrical to the center setting of the obstacle, whereas a certain unsymmetry is to be expected in an actually rolling wheel. According to Figure 17, the increase in wheel force is not great with small obstacles, although it amounts to 15 per cent for the 760 X 100 and the 810 X 125 tires.

With the 40 mm obstacle the discrepancies between the individual tires however, became appreciable. The tire with the smallest increase was the 1,300 X 300 one at  $p = \text{atm.}$ , followed by the 30" X 13" (762 X 330) low-pressure tire with almost the same increase. As the tire width diminishes the rise in wheel force becomes markedly greater and reaches more than 50 per cent for the 760 X 100 tire with 3 to 4 atm. inflation pressure. A test with the same tire but inflated to 1 atm. even revealed a rise of over 60 per cent, which probably is due to the already quite high tire stiffness compared to the low inflation pressure.

One notable feature is the fact that the absolute amount of inflation pressure has no decisive significance, but rather that it is largely a matter of the ratio of height of obstacle  $h$  to tire width  $b$ . In order to bring this out more clearly, Figure 19 shows the maximum increase



in wheel force versus the  $\frac{h}{b}$  ratio for both obstacles and all tires. According to the diagram the  $\frac{h}{b}$  ratio surpasses all other influences to such an extent that the  $\frac{P_{\max}}{P_0}$  values could be approximated by a curve, notwithstanding the difference of the tested tires in design, air pressure, etc.

The conclusions to be drawn therefrom are: First, decide on the necessary minimum elastic travel of the tire for a specific unfavorable ground to insure acceptable rolling over small obstacles. Then the only significance of the inflation pressure is to insure a fitting coordination of the tire to the static wheel load for a given elastic travel (tire width) and a chosen form ratio  $\phi$  (tire diameter). Since in small airplanes it is impossible to obtain large elastic travel, except by low inflation pressure, it forthwith follows that low-pressure tires should be used for small airplanes. To insure identically good qualities for large airplanes, on the other hand, does not necessitate such low inflation pressures. Rather the same good results can be achieved with higher pressures, when providing that the tire width is sufficiently large with respect to the size of the obstacle.

#### 4. PORTION OF TIRE ON SHOCK ABSORPTION OF AIRPLANE

In order to obtain a summary of the part played by the tire in the total shock absorption thus far, we show in Figure 20 the total elastic travel, tire travel, and lastly the elastic travel of the shock absorbers of various airplanes with orthodox landing gears plotted against the wheel load. The figures present averages for high-pressure tires.

Whereas the scattering of the elastic travel of the tire with the given coordination of a certain tire to the gross weight of the airplane is small, that for the elastic travel of the shock absorber is appreciable, since the latter is especially chosen by the designer according to airplane performance.

Aside from the elastic travel, which already reveals a definite picture of the share of the tire on the total shock absorption, the portion of the tire on the energy absorptiveness of the total absorption of shock is likewise of

particular interest. This portion is chiefly dependent on the character of the employed shock absorption mechanism.

The energy absorption of any shock absorber can be defined by the introduction of a ratio  $\eta_1$  of the shock absorption diagram, that shows the ratio of the total available energy of the completely extended shock absorber to the maximum possible energy: maximum load X maximum elastic travel. An approximation of the tire portion on the total shock absorption is the following:

$$\frac{A_g}{A_g + A_{g1}} = \frac{1}{1 + \frac{\eta_1 f_{g1}}{\eta f_g}}$$

This is on the assumption that the tire reaches its maximum travel at the same time as the shock absorber does. In these considerations the relative travel between wheel and airplane mass in direction of the wheel load is always to be used as basis of the elastic travel of the shock absorber. In the event of any appreciable transmission - mostly varying with the elastic travel - between the travel of the axis and that of the shock-absorber struts, the elastic diagram of the shock absorber must be extrapolated to the wheel center. This is of particular importance when defining  $\eta_1$ .

Figure 21 shows the values for the energy absorption quota determined on the basis of the middle curves of Figure 20 and a mean  $\eta = 0.41$  for airplane tires;  $\eta$  varied between 0.36 and 0.45 in the experiments. It is manifest from Figures 20 and 21 that the quota of the tire on the total elastic travel as on the total energy absorption decreases as the wheel load diminishes with the conventional high-pressure tires. So the application of small elastic travel on small airplanes is justified when taking into account the landing impact only and when assuming, at the same time, that the small airplane has a lower landing speed. This, however, is not always the case. Besides, when considering the shape of the ground during rolling of the airplane independent of the airplane size, and which every airplane must pass-over, the reduction of elastic travel in small aircraft leads to inferior rolling characteristics. Thus the study of the tire quota on the total shock absorption again reveals the urgent necessity for improved small tires by increased elastic travel, a need which does not exist so far as the large tires are concerned.

The whole analysis of the elastic properties therefore makes it appear desirable to establish a tire series, beginning with small wheels with low-pressure tires and approximately terminating with increasing wheel size in the high-pressure tire series.

## FACTORS AFFECTING TIRE DIMENSIONS

Before proposing a standard series of tires for airplane wheels, based mainly on the information in the preceding chapters, we touch upon several problems, which likewise exert some influence on the size of the tire. Foremost among these is the resistance to rolling.

### 1. GROUND PRESSURE AND RESISTANCE

The development of the low-pressure tires resulted in markedly lower inflation pressures and through it, in ground pressure, which can be put as being about equal to the inflation pressure. Now the question arises whether such extended drop in inflation pressure with respect to the rolling resistance becomes of such decisive importance, that the choice of inflation pressure is not amenable to satisfactory definition from the points of view advanced in the preceding chapter.

Besides, in the problem of rolling resistance of an airplane tire, we must differential between a number of fundamentally different cases: On very hard, level ground (concrete taxiway for instance) the kneading losses of the tire are decisive for the rolling resistance. High inflation pressure and large diameter are necessary to lower the resistance. From this point of view the high-pressure tire is superior to the low-pressure type.

On very hard, but humpy ground (hard frozen ground with surface very rough) the conclusions as to rolling resistance are similar as for the load absorption when rolling over an obstacle. (Page 14.) The rolling resistance is cut down by a tire of great width. The only relative importance of the inflation pressure is to coordinate a tire with a definite maximum elastic travel to a given wheel load. The ground pressure as absolute value is secondary.

The more the tire gives, the smaller the tire diameter may be.

On very soft ground the rolling resistance is not only dependent on the tire characteristics; on the contrary, there is an added resistance due to sinking even if the ground is perfectly level. In this case the inflation pressure, that is, the ground pressure, is of absolute importance.

The extremely low inflation pressures as already employed for small low-pressure tires, still insure safe rolling on very soft, sumpy or sandy ground. But these cases must be looked upon as out of the ordinary, because on normal airports and emergency landing fields, the experiences of many years with the conventional tires have shown that inflation pressures, i.e., ground pressures as high as 3 to 4 atm. are permissible with appropriate tire dimensions.

From the experiences at hand the following conclusions as to choice of tire dimensions can be drawn. The smallest possible tires are desirable. Reduction of the hitherto large diameter of high-pressure tires must be absolutely accompanied by lower inflation pressure, so as not to increase the rolling resistance on normal landing field ground. The bounds within which to proceed are the old type high-pressure tires on one hand, and the attested Good-year low-pressure tires with low inflation pressure and small diameter on the other.

As to the air resistance, it is pointed out that comparative flight tests with the nonstreamlined wheels 30" x 13" (762 x 330) low pressure and the 810 x 125 high pressure which have about the same wheel load, were slightly in favor of the high-pressure tires. Besides, it should be remembered that with well streamlined landing wheels the resistance of the high-pressure tired wheel is appreciably less. The development of fast airplanes therefore makes entirely new demands on wheel design and tires, so that for the present at least, it is impossible to predict what the final shape of tires actually will be for high speed aircraft. But at the same time it is very appropriate to analyze the experiences gained up to now with high and low pressure tires, and to set up, if at all possible, one standard tire series in order to remove the confusion existing among the users of airplane tires.

## 2. WHEEL LOAD AND LOAD DEFLECTION

The coordination of the static wheel load to any particular size tire is best accomplished by using the static deflection  $\lambda_r$ , called load deflection, occurring under this wheel load. Sometimes the deflection is referred to tire height above rim edge instead of to tire width. We intentionally preferred the latter because it alone represents a typical value from the point of view of shock absorption. To characterize the height above the rim edge it also requires the amount of maximum deflection  $\lambda_g$ , which simultaneously comprises the utilizable elastic travel of the tire.

The choice of permissible load deflection in airplane tires is primarily contingent upon the following: moderate kneading deformation of tire by smooth rolling over level ground, ample clearance between rim and ground for rolling over obstacles, and lastly, a certain accord between the elastic properties of the tire and those of the landing gear shock absorber. In addition to this, the impact factors by definite energy absorption must be reconciled.

The permissible load deflection in automobile tires is small, averaging  $\lambda_r = 0.15$ , although originally it was quite small in airplane tires also, ( $\lambda_r = 0.15$  to  $0.2$ ). But in recent times it was consistently increased, while the inflation pressure was reduced, until today it amounts to  $\lambda_r = 0.3$ , or even more in some cases. The probable reason for this is the gradual breakaway from the typical automobile tire design, with the result that problems of kneading deformation with respect to the demand for a soft elastic adaptable tire were pushed in the background. An example of tire deformation under different deflections is given in Figure 22 for the 30" x 13" (762 x 330) low-pressure tire and the 810 x 125 high-pressure tire. When riding on the rim ( $\lambda_g = 0.72$ ) the low-pressure tire manifests a sharply defined fold in the casing. For full utilization of the energy absorption of such a tire it is advised not to lower the form ratio and the rim diameter to the extremely low figures shown for this tire.

The maximum deflection, so important for the reconciliation of the tire with the landing gear shock absorber, ranged between  $\lambda_g = 0.7$  to  $0.83$  in the examined tires. The lowest figures belong to the tires with small form ratio. However, this is not the general rule, but rather the

result of the chosen rim dimensions. Now when we consider the total energy absorption up to riding on the rim as available, the ratio of the then appearing maximum energy to the simple static wheel load yields the safe impact factor of the tire. The tests conceded impact factor  $n = 5$  to 6 relative to a wheel load corresponding to  $\lambda_r = 0.2$  and  $n = 3$  to 4 relative to a wheel load corresponding to  $\lambda_r = 0.3$ . Admittedly it is desirable to have a higher impact factor for the tire than for the shock absorber, to prevent the former from riding on the rim before the shock absorber attains to its full absorption of energy. On the other hand, an unduly high tire impact factor neither presents any advantage because it does not permit full utilization of the tire volume. The conventional airplane shock absorbers today have a safe impact factor ranging between 2.5 and 3.5, so a tire impact factor of from 3 to 4 should be just about sufficient, i.e. a load deflection of  $\lambda_r = 0.3$  and a maximum deflection  $\lambda_g > 0.7$  can be used as basis for the dimensioning of a standard tire series.

Local hitting of the rim, dreaded so much with automobile tires need not be feared in the airplane tire, even with  $\lambda_r = 0.3$  provided wide widths are used for small tires also.

### 3. INSTALLATION OF BRAKE

Of influence on the tire dimensions, and the rim diameter in particular, is the question as to whether the brake can be conveniently housed in the wheel. Determinative for the dimension are the mechanical and the thermal stresses of the brake.

Mechanical stresses.— According to flight experiences and measurements a brake decelerating force of around 30 per cent of the gross weight of the airplane is amply sufficient to effect a short landing run and acceptable steering brake. (Reference 1.) Thus the braking force per wheel is assumed at

$$P_b = 0.3 P_r$$

This formula yields according to the roll radius of the tire, the braking torque to be supplied by the braking arrangement of the wheel.

Thermal stresses.— The thermal stress of the brake lining can be expressed as the braking power per 1 cm<sup>2</sup> of braking area. The maximum unit brake power is

$$N = \frac{F_b v}{F_b} \frac{\text{mkg}}{\text{s cm}^2}$$

Referring the brake power to the brake drum radius instead of to the roll radius of the tire, yields as second relation per unit brake power of the brake lining:

$$N = \mu q v_T$$

wherein  $\mu$  = mean friction coefficient of brake lining,  $v_T$  = rubbing speed on brake drum and  $q$  = mean surface pressure of lining. How high one may go in the choice of unit brake power, depends on the cooling characteristics of the brake, its location with respect to the tire and the heat characteristics of the brake bands. With 1,300 X 300 cast elektron airplane wheels we obtained unit brake power up to 45 mkg/s cm<sup>2</sup> (2,100 ft.lb/sec. sq.in.) with standard brake bands without excessive heat in brake wheel or damage to brake lining. In contrast to that the braking area of the 30" X 13" (762 X 330) Goodyear low-pressure wheels was so large that not even 10 mkg/s cm<sup>2</sup> (466.6 ft.lb/sec. sq.in.) could be reached in normally braked landings.

Verification on arbitrarily chosen tire dimensions as to the possibility of housing the brake is limited to a verification of the rim diameter, with certain premises for brake drum width and utilization of brake drum area. The braking area is expressed by the total enveloping surface of the brake drum:

$$F_b = \delta \pi D_T b_T$$

$\delta$  is a degree of utilization of the available brake drum area. In two-shoe brakes for instance,  $\delta = 0.4$  to  $0.5$ , and in three-shoe brakes  $\delta = 0.6$  to  $0.8$ . In addition, brake drum width  $b_T$  is referred to the diameter, thus:

$$b_T = \epsilon D_T$$

In internal expanding brakes  $\epsilon$  ordinarily amounts to 0.1 to 0.15. For the hub brake of the tested 30" X 13"

(762 X 330) Goodyear low-pressure tire this figure was  $\epsilon = 1.0$ . Writing the values for  $F_b$  in the equation for unit brake power we finally obtain

$$N = \frac{P_r v}{10.58 \epsilon D_T^2}$$

and for the brake drum diameter:

$$D_T = \sqrt{\frac{P_r v}{10.58 \epsilon N}}$$

These equations are used in the following section, on page 25 to estimate the brake drum diameter.

#### 4. WEIGHT PROBLEMS

The most difficult factor involved when enlarging the tire volume, is undoubtedly the minimum structural weight of the wheel. Reduction in rim diameter permits the design of a compact, solid wheel body. As concerns the tires it is to be noted that any essential increase in volume is followed by a much lower air pressure. This fact should be considered in tire dimensions. The weight of the tire in large volume tires is decisive for the weight of the whole wheel, and it is urgently requested that the designers of airplane tires leave no stone unturned to produce a light yet durable tire series. Fatigue tests on light tires reveal the limit very readily. Any estimate of the weight especially of small tires with large air volume should bear in mind the saving on additional shock absorption attainable by correct utilization of the elastic travel of the tire. A comparison of wheel weights alone therefore reveals quite often a misleading picture.



TABLE III. PROPOSED STANDARD TIRE SERIES WITH GRADED INFLATION PRESSURE FOR AIRPLANE WHEELS

	1	2	3	4	5	6	7	8
Tire Size	mm 570x220 in. 22x8.5	650x250 26x10	760x280 30x11	870x300 34x12	1000x320 40x12.5	1150x340 45x13.5	1300x350 51x14	1400x360 55x14
Wheel load	kg to 400	400-600	600-1000	1000-1600	1600-2400	2400-3500	3500-4700	4700-6000
Inflation pressure $p_0$	atm. to 0.65	0.5-0.8	0.6-1.1	0.9-1.5	1.25-2.0	1.7-2.5	2.2-3.0	2.8-3.6
Form ratio $\phi$	2.6	2.6	2.7	2.9	3.1	3.4	3.7	3.9
Elastic travel under static wheel load								
$f_r$	mm 66	75	84	90	96	102	105	108
Maximum elastic travel								
$f_g$	mm 150	175	195	215	230	250	260	270
Rim diameter $D_F$	mm 190	215	275	345	420	515	640	710
Width of rim wall $b'$	mm 180	200	220	230	230	230	230	230
Height of tire bead $h$	mm 22	23	24	26	28	29	30	32
Brake drum diameter $D_T$	mm 150	175	220	280	330	420	500	570
Brake drum width $b_T$	mm 45	50	60	70	75	75	80	90
Unit brake power $N$	$\frac{\text{mkg}}{\text{s cm}^2}$ 16	19	20	22	26	31	32	32

kg x 2.20462 = lb.      mm x .03937 = in.      mkg/s cm<sup>2</sup> x 46.6644 = ft.lb./sec.sq.in.

## PROPOSED NEW TIRE SERIES FOR AIRPLANE WHEELS

On the basis of the foregoing we have worked up a proposed new tire series which, as standard series, is to combine the advantages of both the low-pressure and of the high-pressure tires. Figure 23 shows the over-all dimensions of this proposed standard series, along with the data for tire cross section, rim, and brake drum. The principal dimensions along with other related data are appended in Table 3.

A few explanations follow: The establishment of new tire series should be restricted to as few sizes as possible. Eight tires should be sufficient for the range of wheel loads existing in airplane design. For small airplanes a still smaller tire is probably suitable.

In setting up the series the fact was kept in mind that the chief purpose of the tire is to overcome obstacles on the ground. To this end an elastic travel of  $f_g = 200$  to 250 mm is recommended. Unfortunately however, it is not possible to attain to a minimum of 200 mm travel for the small airplane, because it would mean unduly large tire volume with respect to the airplane size. For that reason the maximum elastic travel of the smallest tire was put at  $f_g = 150$  mm.

As form ratio  $\phi$  we chose a stage between 2.6 for the smallest tire, and 3.9 for the largest. For very large high-pressure tires a  $\phi = 4$  has proved very acceptable. As lower limit  $\phi = 2.2$  has already been obtained, but this figure appears unduly low from the point of view of unfavorable tire deformations under large deflection and the very small rim diameters. As minimum we chose  $\phi = 2.6$ , because rolling circle diameters still occur, which permit safe landing with bursted tire, even in cases where the pilot is ignorant of it.

For the coordination of the wheel load a  $\lambda_r = 0.3$  load deflection was chosen. (See page 20.) The assumed wheel loads, which permit a favorable coordination to the usual gross weights of modern airplanes, the form ratio  $\phi$  and deflection  $\lambda_r$  yield forthwith the grading of the inner pressure  $p_0$  on the basis of the analysis expounded in section on page 9. It is advisable not to raise the pressure much above 3.5 atm. even for large wheels, in order to avoid too much ground pressure when the ground is soft. If

the ground is very soft, as on certain commercial air lines, the design of oversize tires with low inflation pressures for the same rims might be advisable.

The cited rim and brake drum dimensions are merely aids for the estimation of the tire series without serving as absolute prototype. The rim diameter was chosen on the basis of the usual figures of today (see fig. 24) and specifically with a view to brake installation, but at the same time small enough so that the maximum possible tire deflection affords at least  $\lambda_g = 0.7$ , to insure full use of the tire volume.

The demands on the brake are high, because in spite of the chosen large rim diameters the space for the brake drum and mounting of the brake mechanism is very restricted. As a result only such brakes come into question which permit the use of the greatest possible portion of the brake drum area. In order to facilitate the estimation of the braking effect, we included in Table III the unit brake power of the brake linings for the chosen drum dimensions, which were computed for a rolling speed of 20 m/s by first full braking effect and a  $\delta = 0.7$  degree of utilization of the brake drum (corresponding approximately to a three-shoe brake). The unit brake power with the small tire, whose wheel body is especially small, and does not evacuate the heat readily, begins with a low figure and rises to figures for large tires which are well within control with light metal wheels.

The hub dimensions in Figure 23 are merely intended to make the comparison of the tire series with the conventional high-pressure tires easier, and should in no way be construed as pattern for the design of wheel hubs. The hub dimensions correspond to the conventional coordination of today to the wheel load of German high-pressure wheels.

The grading of the proposed standard series becomes readily manifest from Figures 25 and 26, while Figure 27 shows the maximum elastic travel of the proposed series along with several others. The old high-pressure tires yield a slightly curved rise in available elastic travel under increasing wheel load. The more recently proposed low-pressure tire series with 0.5 to 1.5 atm. inflation pressure admittedly proffer a decided improvement in tire travel, but they leave untouched the very marked difference in absolute elastic travel between small and large wheels, which is in no wise justified for the rolling. The primary purpose of the tire is "cushioning in rolling" and not

"cushioning of landing shock." The energy of one single severe landing shock can be better absorbed i.e., with greater damping, much less expenditure of weight and air resistance by a modern shock absorbing strut than is possible by a very large size tire. In accordance with this it is attempted with the standard series to utilize the advantages accruing from the low-pressure tire for small airplanes, but by a gradual change in dimensions and corresponding grading of inflation pressure to attain to light, large tires with relatively small air volume and low air resistance.

### PROSPECTS

It is impossible to bring all the tire qualities that have some bearing on its practical use within exact mathematical treatment. It was not the object of this work to simply compute the best design shape. Compromises must be made. The primary motive of this analysis of tire sizes was rather to bring the discussion low-pressure versus high-pressure tires to a uniform basis and to find a way to judge tires of any size for airplane wheels. It is hoped that the questions touched upon here will stimulate discussion and comment. In particular, the experience of the different countries that have been engaged in the development of tire series for airplane wheels, should prove very interesting. It would be very gratifying, indeed, if the discussion would ultimately lead to an international standard for tire sizes and wheel hubs.

Translation by J. Vanier,  
National Advisory Committee  
for Aeronautics.

### REFERENCE

1. Michael, Franz: Experiments with Airplane Brakes.  
T.M. 636, N.A.C.A., 1931.



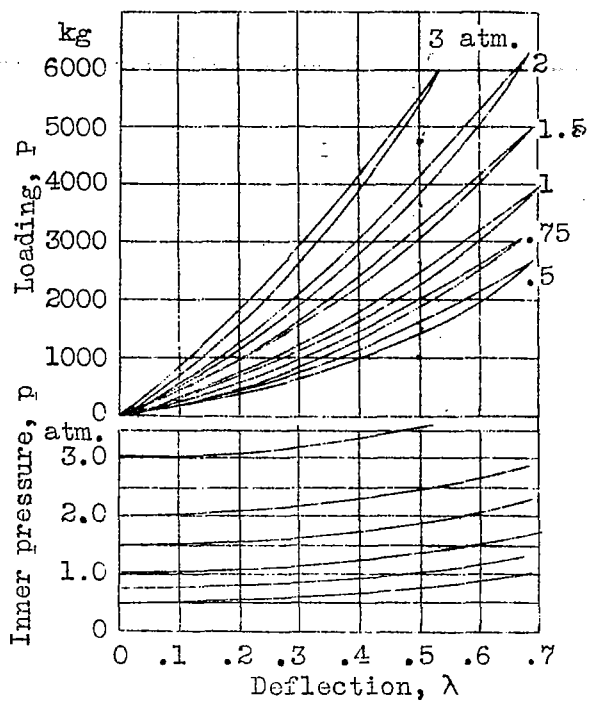


Fig. 5 Load absorption and inner pressure rise of 30" x 13" (762 x 330 mm) American tire at various inflation pressures plotted against deflection  $\lambda$ .

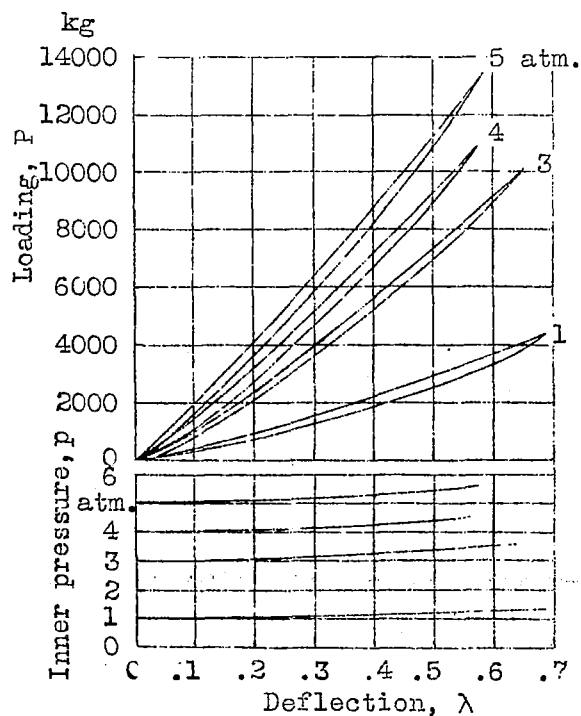


Fig. 6 Load absorption and inner pressure rise of German 1300 x 300 tire under different inflation pressures plotted against  $\lambda$ .

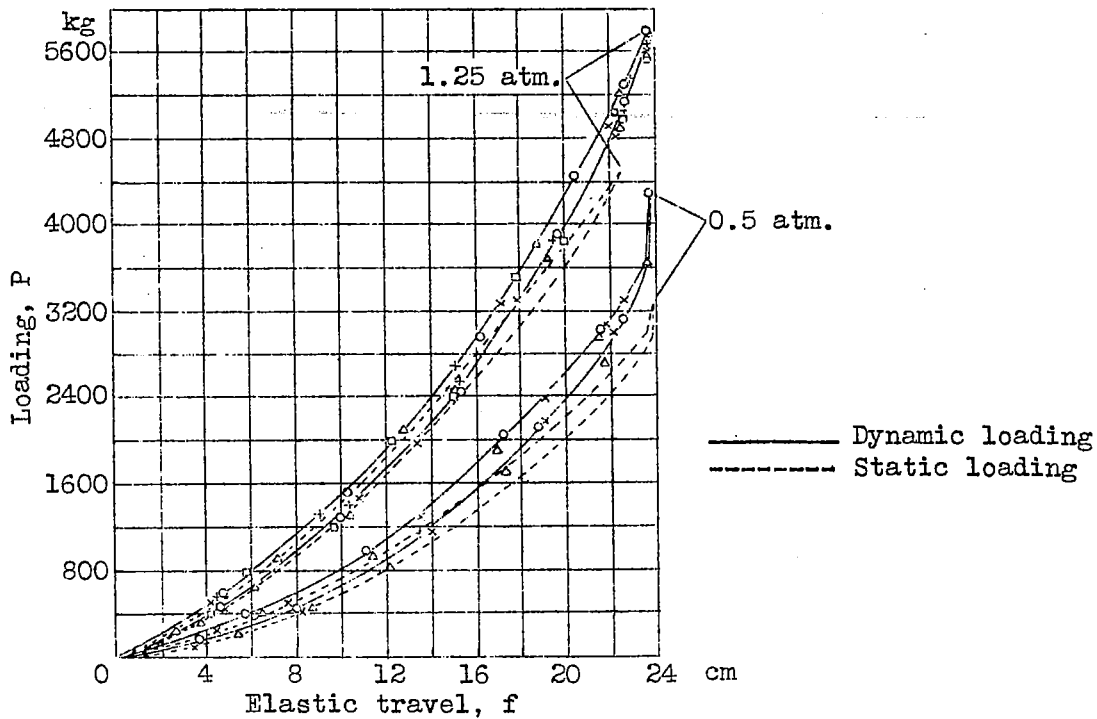


Fig.7 Load absorption of American 30"x13" (762 x 330 mm) tire in drop test at different impact velocities plotted against elastic travel f .

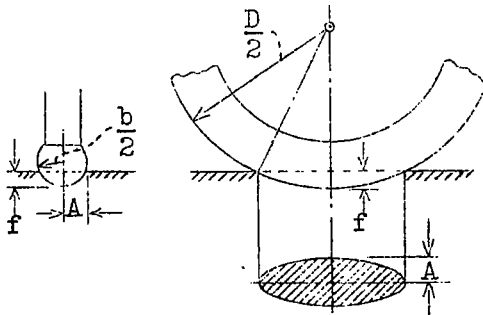


Fig.8 Approximation ellipse of area of contact.

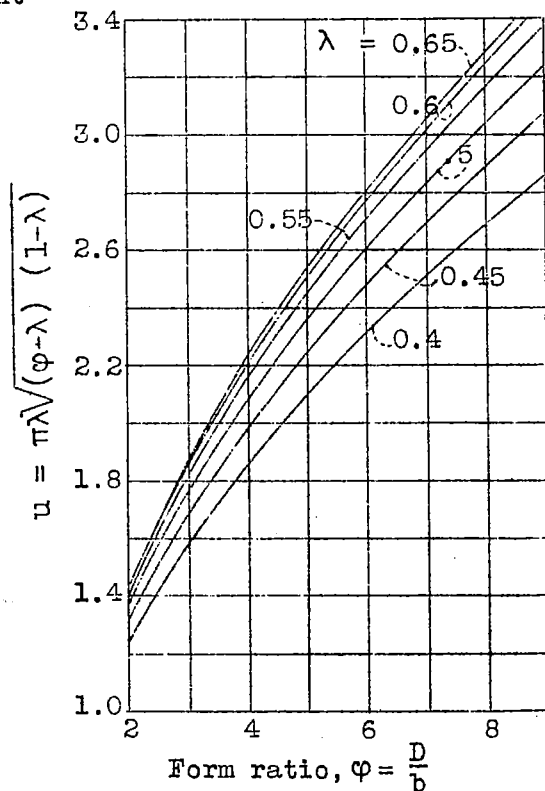


Fig.9 For calculating ellipse areas,  $F_e = ub^2$  .

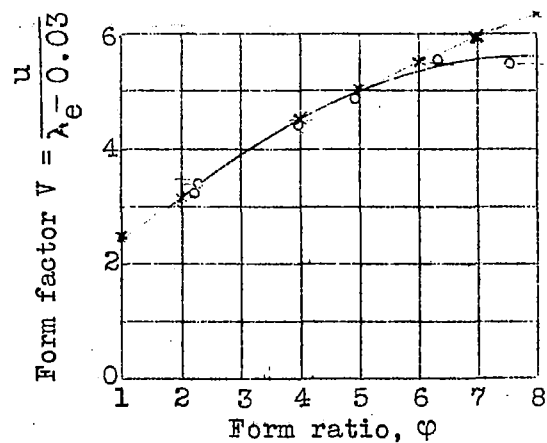


Fig.10 Form factor  $V$  versus form ratio  $\phi$  .

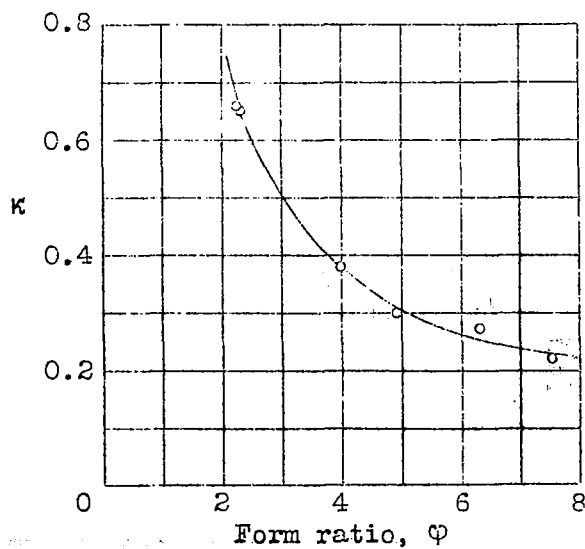
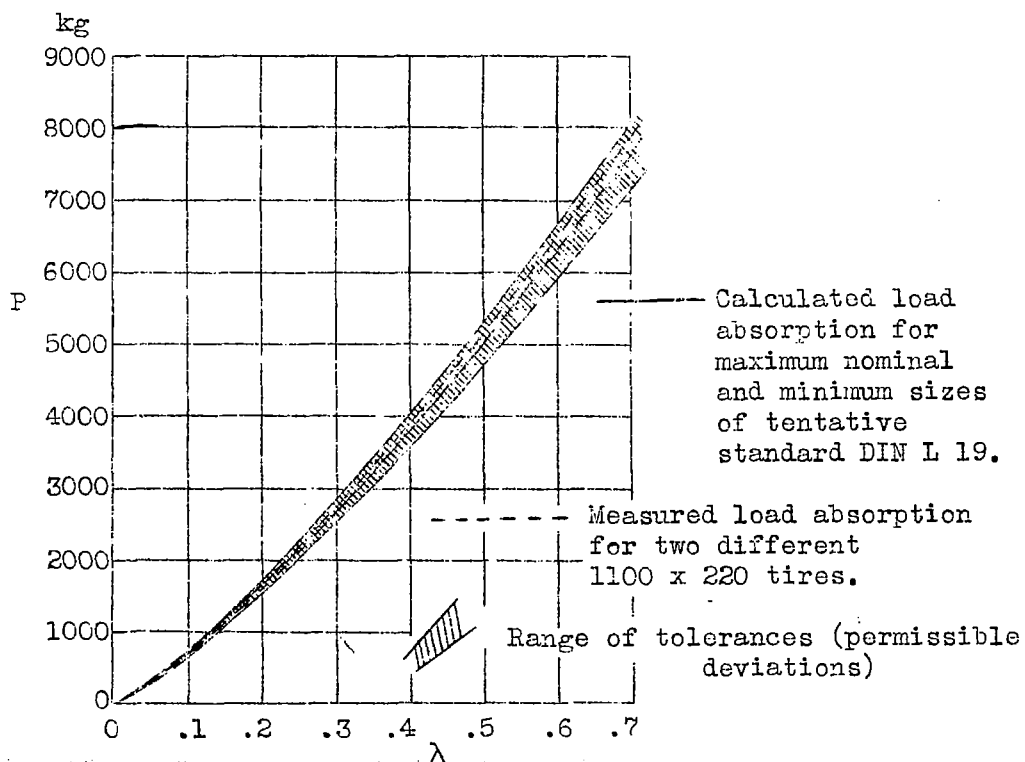
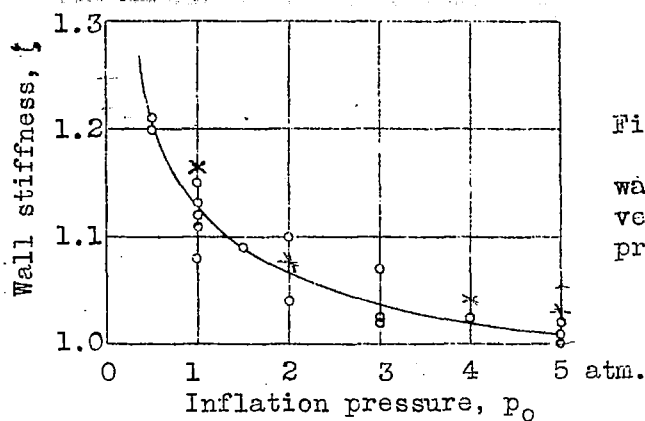


Fig.11 Definition of the inner pressure rise  $\kappa$ , versus form ratio  $\phi$ .





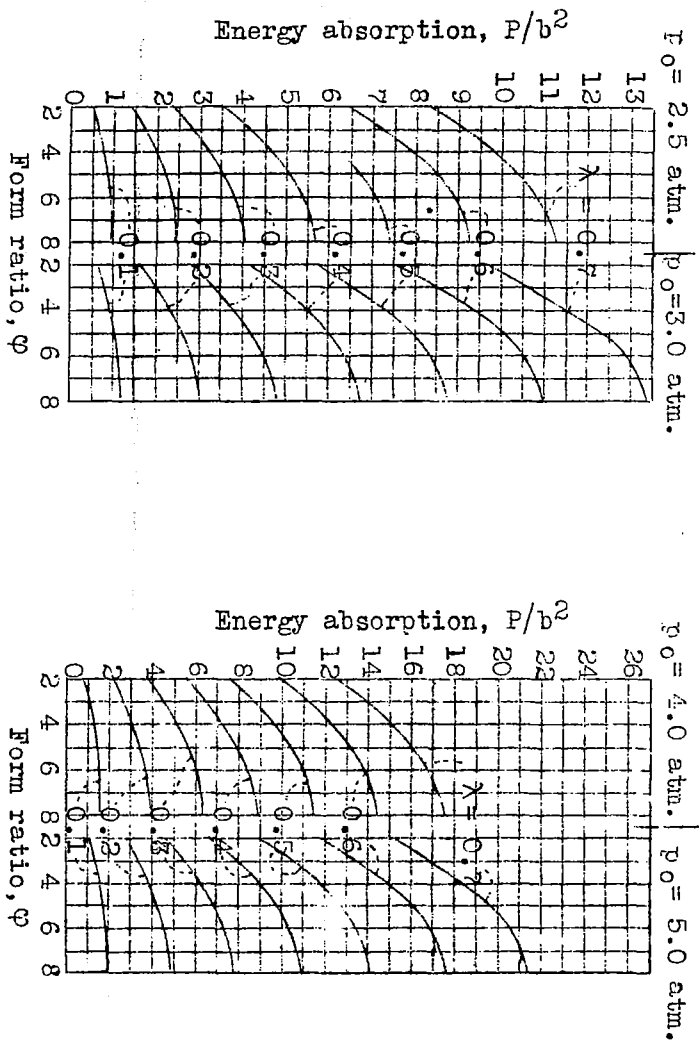
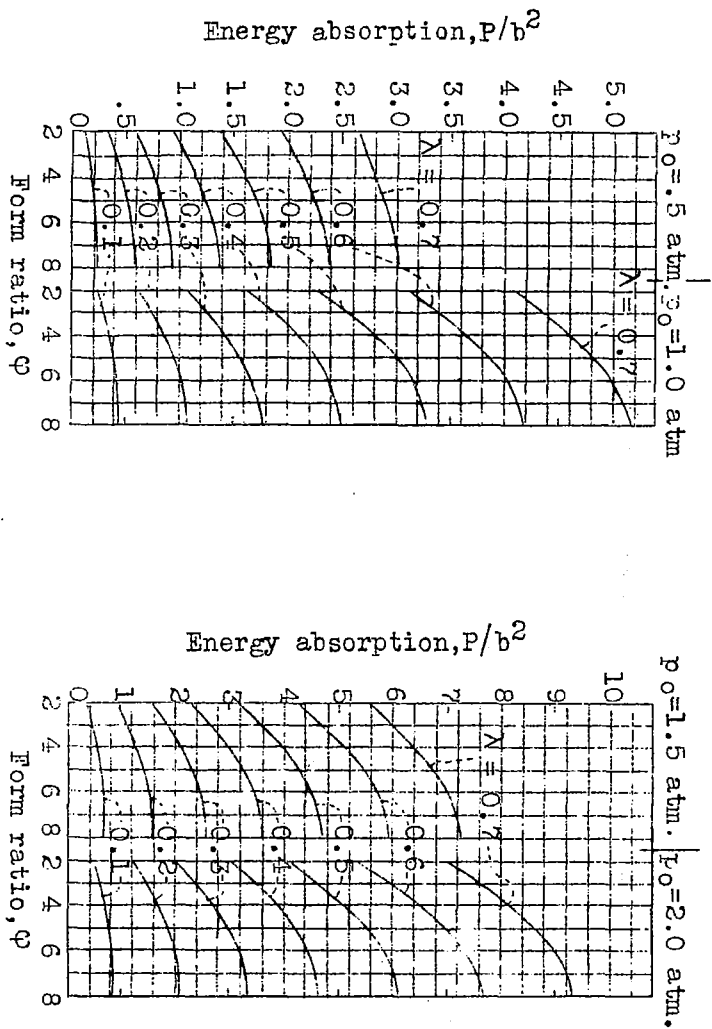


Fig.14 Determination of load absorption.



Fig.15 Loading corresponds to  $\lambda_r = 0.3$ ; photograph 2 and 2' show obstacle setting for maximum wheel load increase. In 5 and 5' the obstacle is in the center position vertically below the wheel axle; see also the areas of contact marked 2 and 2' in Fig.16 belonging to these tires.

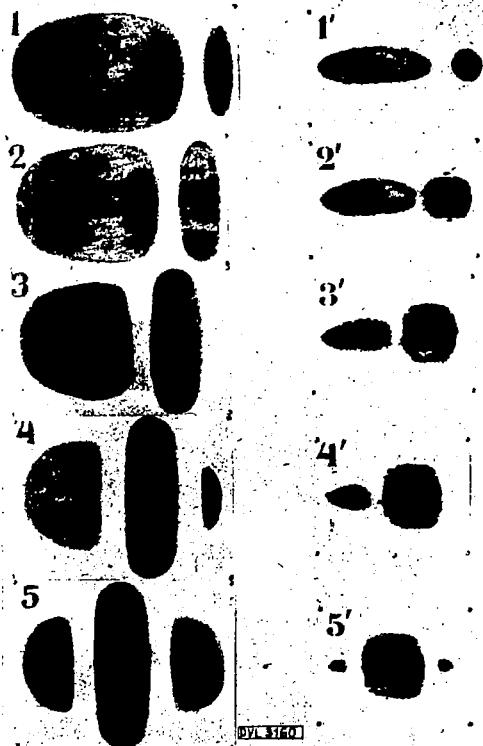
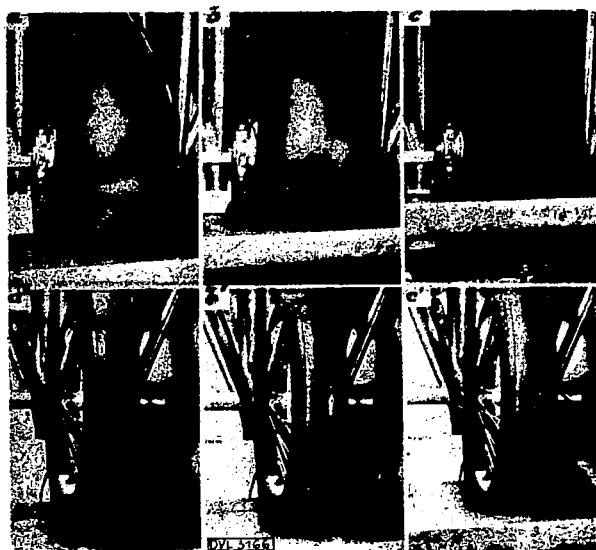


Fig.16 Areas of contact in load test corresponding to Fig.15; 1 to 5 for 30" x 13" low-pressure tire and 1' to 5' for 810 x 125 high-pressure tire. The maximum rise in wheel force does not lie with center setting (5, 5') but rather with 2, 2' obstacle setting.



(30"x13" = 762 x 330 mm)

Fig.22 Deformation of 30" x 13" and 810 x 125 tires under loading corresponding to deflection

$$\lambda = \lambda_r = 0.3 \text{ (a and a')}$$

$$\lambda = 0.5 \text{ (b and b')}$$

when riding on rim, i.e. when

$$\lambda = \lambda_g = 0.72 \text{ (c)}$$

$$\lambda = \lambda_g = 0.8 \text{ (c')}.$$

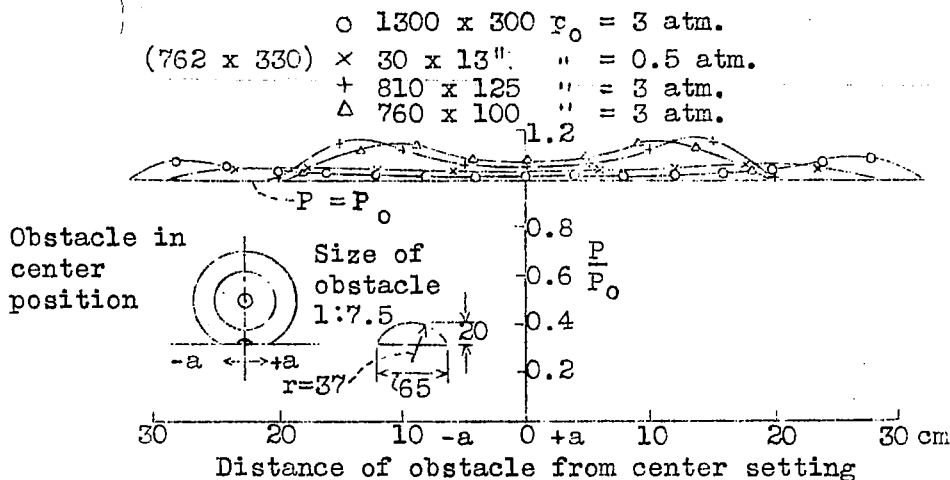


Fig.17 Rise in wheel force  $P/P_0$  when rolling over a 20 mm high obstacle, assuming the rolling is infinitely slow and elastic travel  $f =$  constant, is forced.

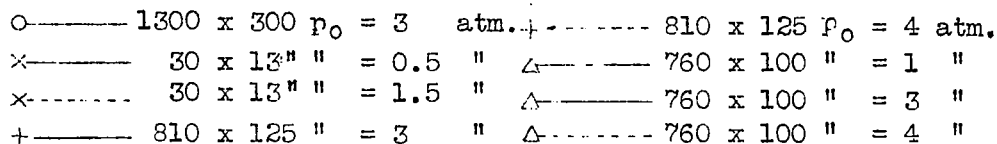


Fig.18 Rise in wheel force  $P/P_0$  when rolling over a 40 mm high obstacle, assuming the rolling is infinitely slow and elastic travel  $f =$  constant, is forced.

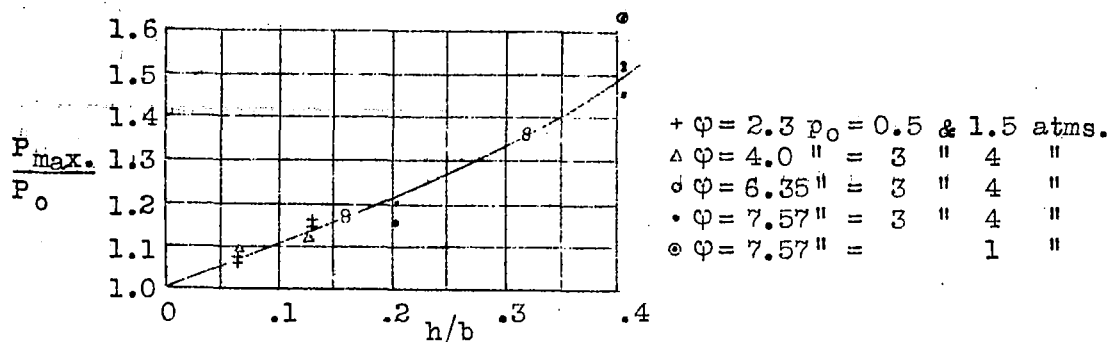


Fig. 19 Maximum rise in wheel force  $\frac{P_{\max}}{P_0}$  versus obstacle height/tire width ratio.

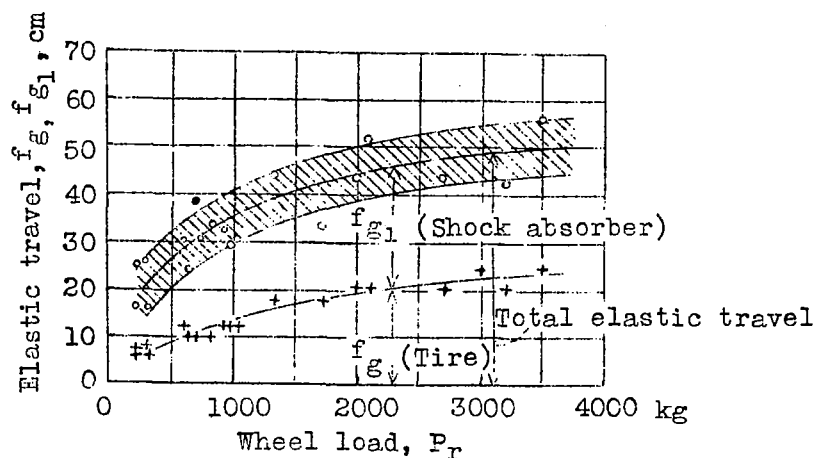


Fig. 20 Elastic travel of conventional landing gears versus static wheel load when using high pressure tires.

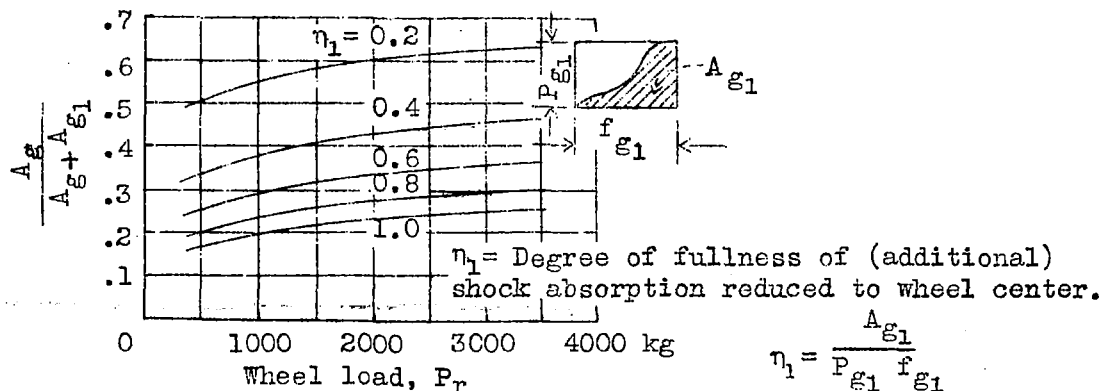


Fig. 21 Quota of energy absorption of tire on the total energy absorption of landing gear versus static wheel load. The maximum elastic travel for tires and shock absorber corresponds to the middle curves of Fig. 20.

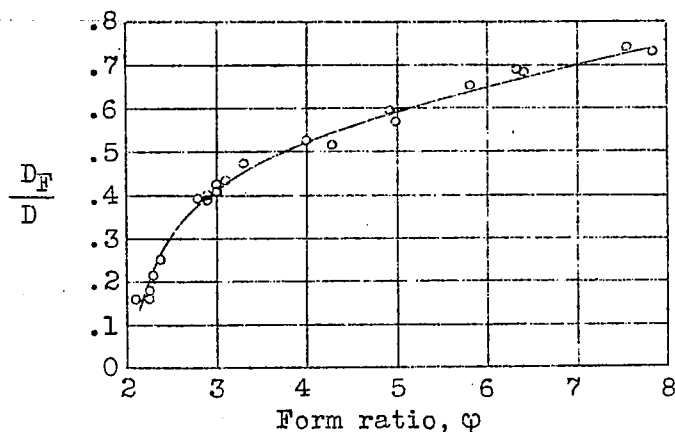


Fig. 24 Conventional rim diameters referred to  $D$  plotted against form ratio  $\phi$ .

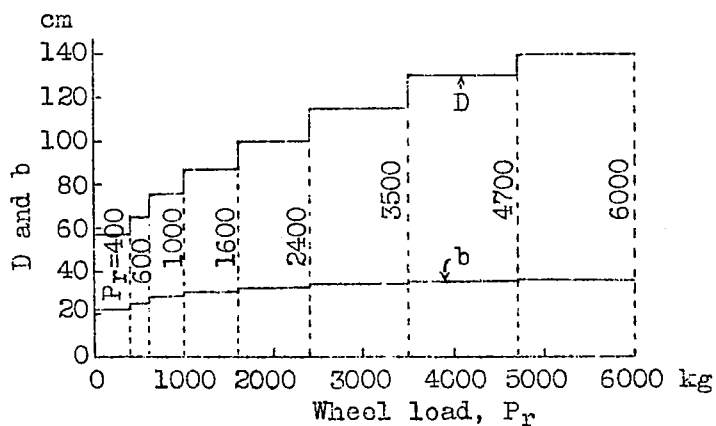


Fig. 25 Graduation of tire diameter and tire width of the proposed series plotted against static wheel load  $P_r$ .

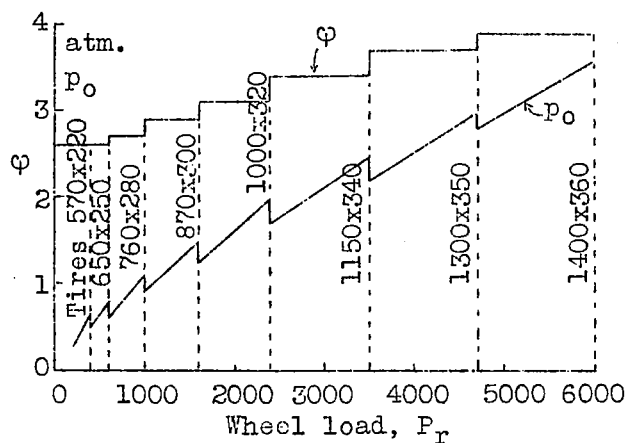


Fig. 26 Graduation of form ratio  $\phi$  and inflation pressure of proposed tire series versus static wheel load.

- $\nabla$  German high-pressure tires       $\times$  American low-pressure tires (\*)  
 $\circ$  American " " " "       $\square$  Goodyear " " "  
 $+$  English " " " "       $\Delta$  Proposed standard series  
 (\*) According to S.A.E. handbook, supplement July 1931.

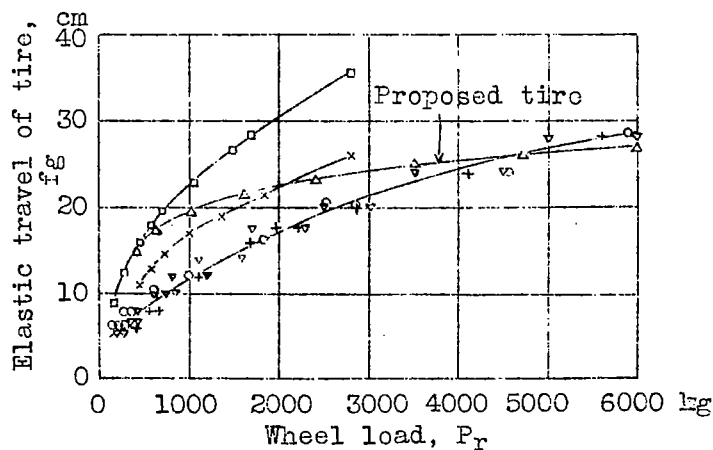


Fig. 27 Maximum elastic travel of tire versus static wheel load for different tire series.

LANGLEY RESEARCH CENTER



3 1176 00189 6035